INSTITUTE OF PHYSICS PUBLISHING SUPERCONDUCTOR SCIENCE AND TECHNOLOGY

Supercond. Sci. Technol. **19** (2006) 1124–1129 doi:10.1088/0953-2048/19/11/006

Thickness dependence of pinning mechanisms in granular Nb thin films

S L Prischepa[1,2], D Montemurro[1], C Cirillo[1], C Attanasio[1], M Salvato[3,4], V Merlo[3], A N Lykov[5] and A Yu Tsvetkov[5]

[1] CNR/INFM Laboratorio Regionale SuperMat and Dipartimento di Fisica 'ER Caianiello', Università degli studi di Salerno, I-84081 Baronissi (Sa), Italy
[2] Belarus State University of Informatics and Radioelectronics, P Brovka street 6, 220013 Minsk, Belarus
[3] Dipartimento di Fisica, Università degli Studi di Roma 'Tor Vergata', I-00133 Roma, Italy
[4] CNR/INFM Laboratorio Regionale SuperMat, I-84081 Baronissi (Sa), Italy
[5] Laboratory of Superconductivity, P N Lebedev Physical Institute RAS, Leninsky prospekt 53, 119991 Moscow, Russia

Received 26 June 2006, in final form 10 September 2006
Published 27 September 2006
Online at stacks.iop.org/SUST/19/1124

Abstract
We have investigated the influence of thickness on the pinning properties of granular sputtered Nb films in a parallel magnetic field. The presence of a crossover in the pinning mechanisms at some critical thickness d_c was established. Below d_c the pinning is due to individual vortices. Above d_c the commensurability between the vortex period and the film thickness occurs, causing a large increase in the critical current density due to surface pinning. It is shown that, in the vortex-free limit, when the critical current is determined by the depairing current, the effect of the commensurability is not present.

1. Introduction

The dependence of the superconducting properties on the thickness d of Nb thin films has been a widely studied problem [1–5]. For example, it has been demonstrated that d influences the values of the critical current density, J_c, and determines the pinning mechanisms in the sample [6]. A change in the sample thickness can, for instance, result in a crossover in the pinning mechanism [6]. In particular, the case of a superconducting film in a magnetic field directed along its surface has also been considered. In this case, if the interaction between vortices is stronger than the interaction with pinning centres, then the vortex lattice is weakly distorted and behaves coherently in a macroscopic volume $V_c = R_c^2 L_c$, where R_c and L_c are the transverse and the longitudinal correlation lengths, respectively. In this case, collective pinning is realized and in principle J_c does not depend on d. When the sample thickness is decreased the vortex lattice becomes less elastic [7]. The correlation volume diminishes until, for $d < R_c$, the reduced flux bundle volume $V_c = L_c R_c^2 = L_c d^2$ changes very rapidly with d towards the volume of a single vortex. This causes the crossover of the pinning mechanism from collective to individual. Considering that, for a thickness $d < \lambda$, the distance of intervortex interaction, λ, should be substituted by $d/\pi \ll \lambda$, the critical thickness, d_c, at which the crossover is realized can be estimated to be [7]:

$$d_c = 35\lambda^2 \left[\frac{J_c^{bulk}}{cH\xi}\right]^{1/2}, \qquad (1)$$

where c is speed of light, J_c^{bulk} is the critical current density of the bulk sample at the magnetic field H, and ξ is the coherence length. For Nb, estimations give $d_c \approx 20$–40 nm.

However, the behaviour of the vortex matter depends not only on the vortex–vortex repulsion but also on the interaction between vortices and pinning potentials. Pinning mechanisms and critical current densities are very sensitive to the presence and the dimension of defects as well as to the film microstructure (grain boundaries, microcracks, etc). The interaction between the vortices and the defects influences the absolute value of J_c, its magnetic field dependence and the pinning force $F_p(H) = |\boldsymbol{J}_c \times \boldsymbol{H}|$ [8]. When the period of the vortex lattice is almost equal to the period of inhomogeneities, the vortex mobility can be lowered and the J_c values grow at a certain magnetic field (the so-called peak effect [9]). Moreover, if the microstructure of the superconducting film is columnar, peculiar properties of $J_c(\Theta)$ are observed (Θ is the angle between the magnetic field and the film surface): for instance,

 © 2006 IOP Publishing Ltd Printed in the UK

Table 1. Measured and calculated parameters of the samples. (Note: NR = not revealed.)

d (nm)	T_c (K)	$H_{c2\parallel}$ (T) at 4.2 K	$\rho_{10\ K}$ ($\mu\Omega$ cm)	Roughnes Nb (nm)	Thickness Nb_2O_5 (nm)	Roughness Nb_2O_5 (nm)	Roughness Si (nm)	Lateral correlation length (nm)
16.0	5.85	5.8	38.8	0.27	2.1	0.7	0.8	40
24.8	6.15	3.5	32.2	1.3	NR	NR	0.1	234.5
32.0	6.45	3.25	31.0	1.6	NR	NR	0.4	249.7
50.0	7.50	2.5	9.0	1.8	NR	NR	0.2	378.0
81.5	7.45	1.9	18.4	2.2	NR	NR	1.4	149.9
103.1	7.25	1.9	23.7	2.5	NR	NR	0.5	

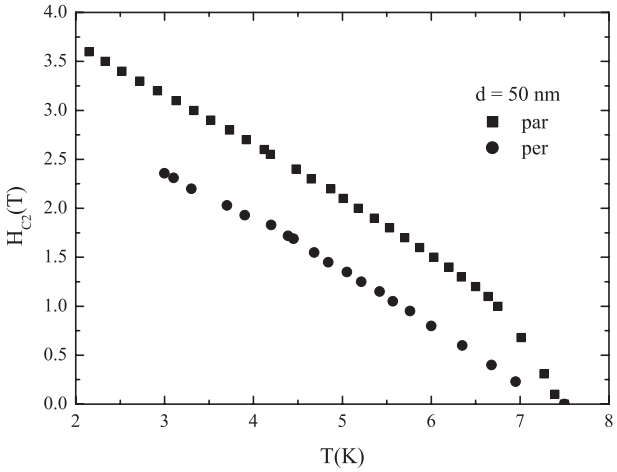

Figure 1. Upper critical magnetic fields, H_{c2}, versus temperature for perpendicular (circles) and parallel (squares) orientation of the magnetic field for the sample with $d = 50$ nm.

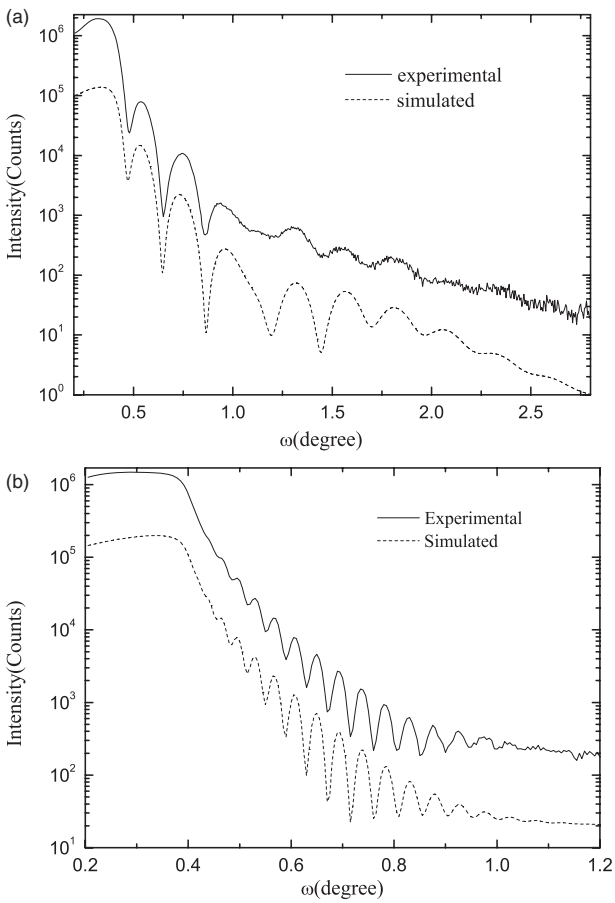

Figure 2. Experimental and simulated reflectivity spectra of Nb samples with (a) $d = 16$ nm and (b) $d = 81.5$ nm.

the way in which J_c approaches $\Theta = \pi/2$ and the fact that the maximum of J_c is observed at Θ is slightly different from zero [4, 5, 7, 10–12].

In this work the $J_c(d, H)$ dependencies of granular Nb sputtered films in parallel magnetic field are presented. The results are interpreted in terms of a crossover in the pinning mechanism, as a function of the films thickness. The comparison between the experimental results and the theoretical simulations, performed in the vortex-free limit, confirms the presence of commensurability effects in thick films.

2. Structural and transport properties

Nb films were grown on Si(100) substrates by dc sputtering. In total, six films with thicknesses of 16.0, 24.8, 32.0, 50.0, 81.5 and 103.1 nm were deposited. A standard lift-off technique was used to define the sample's geometry, consisting of strips 10 μm wide and 90 μm long. The deposition rate was calibrated by x-ray reflectivity measurements. Critical current values were determined from current–voltage characteristics measured by a pulsed technique. The pulse length was 30 ms. The electric field criterion for J_c definition was $E_c = 10^{-2}$ V m^{-1}. The magnetic field was always applied parallel to the film surface and perpendicular to the current direction.

The temperature dependence of the perpendicular, $H_{c2\perp}(T)$, and of the parallel, $H_{c2\parallel}(T)$, upper critical magnetic fields were also measured on all the samples. From $H_{c2\perp}(T)$ we extracted the Ginzburg–Landau coherence length value ξ_{GL} [13]. The upper critical field was obtained at the onset of the $R(H)$ curves registered at different temperatures (here R is the resistance). Temperature stabilization was better than 10^{-2} K. The value of $\xi_{GL}(0)$ was around 7.4 nm for all the samples, which gives the BCS coherence length $\xi_0 = (2/\pi)\xi_{GL} = 4.7$ nm. The H–T plot (both for parallel and perpendicular magnetic field orientation) for the sample with $d = 50$ nm is shown in figure 1. The values of $H_{c2\parallel}$ at 4.2 K for all the samples are reported in table 1.

The microstructure of all the deposited samples was investigated by means of both low- and high-angle x-ray analysis. Results of the experimental reflectivity spectra for samples with $d = 16$ and 81.5 nm are shown in figures 2(a) and (b) together with the results of simulations obtained using

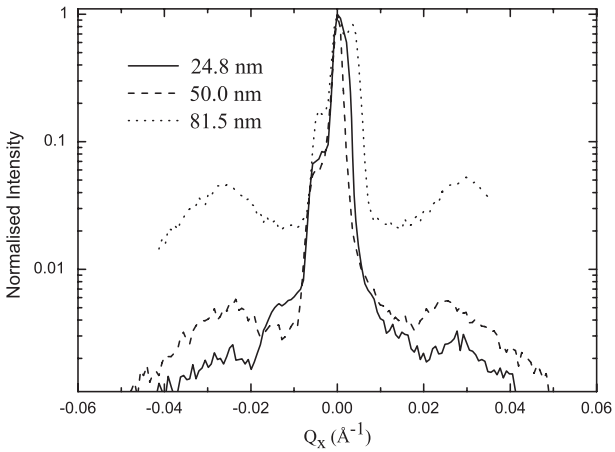

Figure 3. Experimental reflectivity rocking curves of the samples with $d = 24.8$, 50 and 81.5 nm. The lateral wings indicate the presence of correlated roughness along the growth direction.

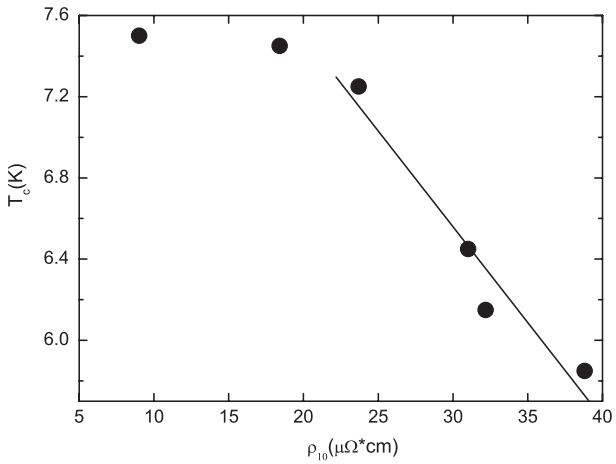

Figure 4. Dependence of the critical temperature, T_c, on the low-temperature resistivity, ρ_{10}. The solid line represents the slope $dT_c/d\rho \approx -0.09$ K $\mu\Omega^{-1}$ cm^{-1} for $d > 20$ nm.

the Parrat and Nevot–Croce formalism [14, 15]. Apart from the difference in distance between the peaks due to the different thicknesses, the reflectivity profile of figure 2(a) presents an over-modulation at $\omega \approx 1.2°$, which suggests the presence of an over-layer. The theoretical simulation shown in the same figure, obtained using the standard values for the mass density of both substrate and film, gives a 2.1 nm Nb_2O_5 over-layer on the top of the Nb surface. On the other hand, for thicker films the reflectivity spectra were well fitted without the presence of Nb oxide layers (figure 2(b)). Table 1 also reports the values of roughness of the film surface obtained with the same fitting procedure, showing that surface roughness increases on increasing the film thickness.

Rocking curves acquired on the second reflectivity peak are shown in figure 3 for three samples with $d = 24.8$, 50 and 81.5 nm. Generally speaking, the rocking curve on a reflectivity peak gives information on the lateral and vertical correlation of the roughness. The full width at half maximum (FWHM) (ΔQ_x) of the central peak is related to the lateral correlation length by the relation $L = 2\pi/\Delta Q_x$ whereas the presence of the lateral wings indicates that the roughness is correlated along the growth direction [16]. The relative intensity of the lateral wings, with respect to the central peak, indicates the degree of correlated roughness in the growth direction. In our case, the L values are calculated and reported in table 1. The presence of the lateral wings indicates that the substrate roughness propagates along the film thickness. The data reported in figure 3 show that the roughness is more strongly correlated for thicker films. Therefore, on increasing the layer thickness, more roughness is present on the surface, as expected, and this roughness also appears to be more correlated. The data in table 1 also suggest that the correlation along the lateral direction does not depend on the film thickness. This is expected, because the nucleation growth proceeds by coalescence along the substrate surface and the growth front can easily be destroyed by the presence of any kind of inhomogeneity.

High-angle x-ray analysis (not shown here) is typical for Nb and indicates that the Nb films grow (110) oriented in the growth direction but textured in the plane of the substrate. Moreover, vertical and lateral grain dimensions calculated from the FWHM of the (110) Nb peak and of the rocking curve of the (110) Nb peak respectively, were both of the order of 10 nm, independent of the film thickness. No peaks related to the presence of Nb oxide layers were detected by high-angle x-ray measurements, although reflectivity spectra show that a Nb_2O_5 layer is formed at least in the thinnest Nb film. This is probably because, if present, the Nb oxide layer is too thin to be detected by our experimental set-up.

Then we may conclude that we obtained Nb polycrystalline films with grain dimensions of the order of 10 nm, a surface roughness of the order of nanometres, and that a thin Nb oxide is present only on the surface of the thinnest Nb film.

In figure 4 we show the dependence of the critical temperature, T_c, on the resistivity value at $T = 10$ K, ρ_{10}. The relatively high values of ρ_{10} confirm the high granularity of our samples. From figure 4 it follows that, in the region 20–40 $\mu\Omega$ cm, the derivative $dT_c/d\rho \approx -0.09$ K $\mu\Omega^{-1}$ cm^{-1}, which is in very good agreement with the results related to the T_c investigation of Nb films with controlled disorder ($dT_c/d\rho \approx -0.10$ K $\mu\Omega^{-1}$ cm^{-1}) [17, 18]. Strong granularity also explains the relatively low T_c values for our films.

3. Results and discussion

An important consequence of high granularity is the anomalous angular dependencies of critical currents [5, 10, 11, 19]. Grain boundaries could be considered as strong pinning centres when the field is oriented perpendicular to the sample surface, leading to an increase in J_c for $\Theta = \pi/2$ [9]. In figure 5 we present the result of the $J_c(\Theta)$ measurements for two samples, with $d = 103.1$ nm and $d = 16$ nm. Measurements have been made at $T = 4.2$ K by rotating the samples at a fixed magnetic field value, $\mu_0 H = 0.5$ T. The thicker sample shows an increase in J_c, while Θ goes towards $\pi/2$. The height of this peak is smaller than at $\Theta = 0$ and it is much more spread. On the other hand, the peak at $\Theta = \pi/2$ is absent for the sample with $d = 16$ nm, in spite of the larger ρ_{10} value for this sample. The explanation for this behavior is related to

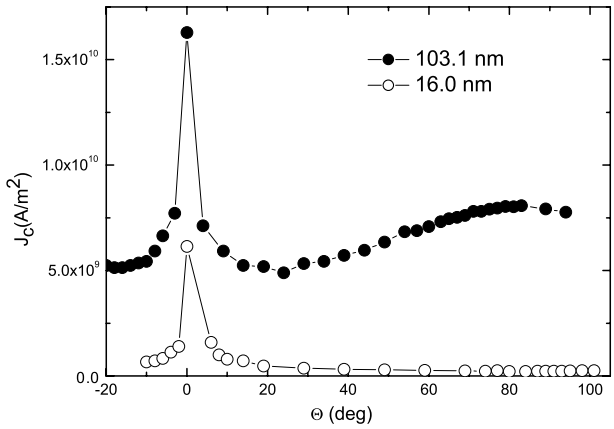

Figure 5. Angular dependence of the critical current density, J_c, at $T = 4.2$ K and $\mu_0 H = 0.5$ T for samples with $d = 16$ nm and $d = 103.1$ nm.

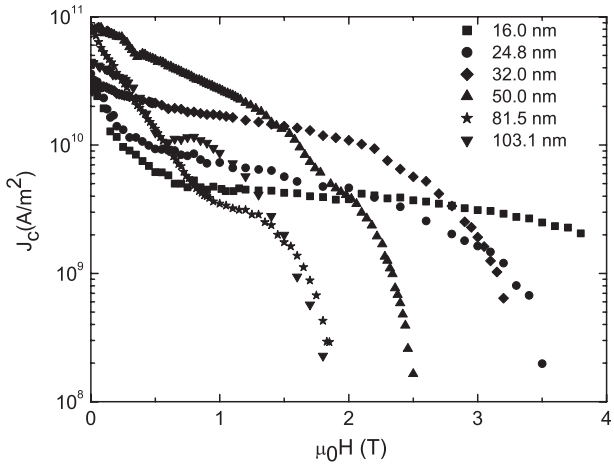

Figure 6. Critical current density, J_c, versus parallel magnetic field, $\mu_0 H$, for all the samples at $T = 4.2$ K.

the smaller values of the lower critical perpendicular magnetic field, $H_{c1\perp}$, for thinner films due to the larger demagnetization factor [13]. It means that, for $d = 103.1$ nm, vortices at $\mu_0 H = 0.5$ T penetrate mostly in between grains and are well pinned, while for $d = 16$ nm the sample becomes transparent for the same magnetic field value. In this case, vortices are also situated inside grains, giving rise to lower J_c values and to the absence of the J_c increase at $\Theta \to \pi/2$ [19].

In figure 6 we show the experimental $J_c(H)$ dependence of the Nb films at $T = 4.2$ K, which corresponds to a reduced temperature, $t = T/T_c$, ranging from 0.56 to 0.72. In figure 7 we show the $J_c(d)$ dependence for all the measured samples at three different reduced magnetic fields, $h = H/H_{c2\|} = 0.65$, 0.75, and 0.85. In all cases, the behavior is non-monotonic, showing a first increase in J_c and then a decrease as d grows. The maximum of J_c is reached for the sample with $d = 32$ nm. Analogous dependencies have also been observed in different superconducting systems [7, 20, 21].

In order to get deeper insight into the problem, we investigated the pinning forces in the two different regions

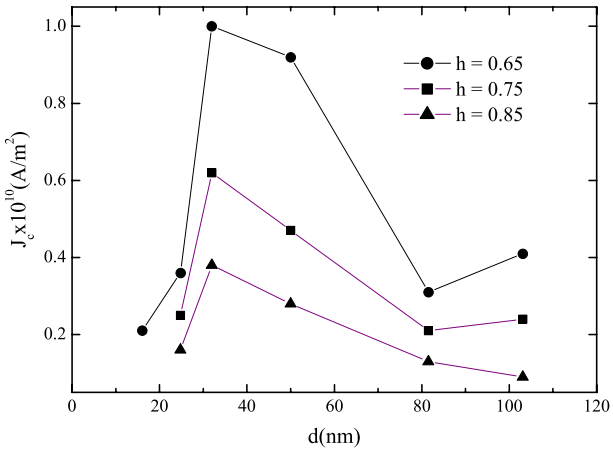

Figure 7. Critical current density, J_c, versus Nb thickness, d, at the reduced parallel fields $h = 0.65$ (circles), 0.75 (squares), 0.85 (triangles).

(This figure is in colour only in the electronic version)

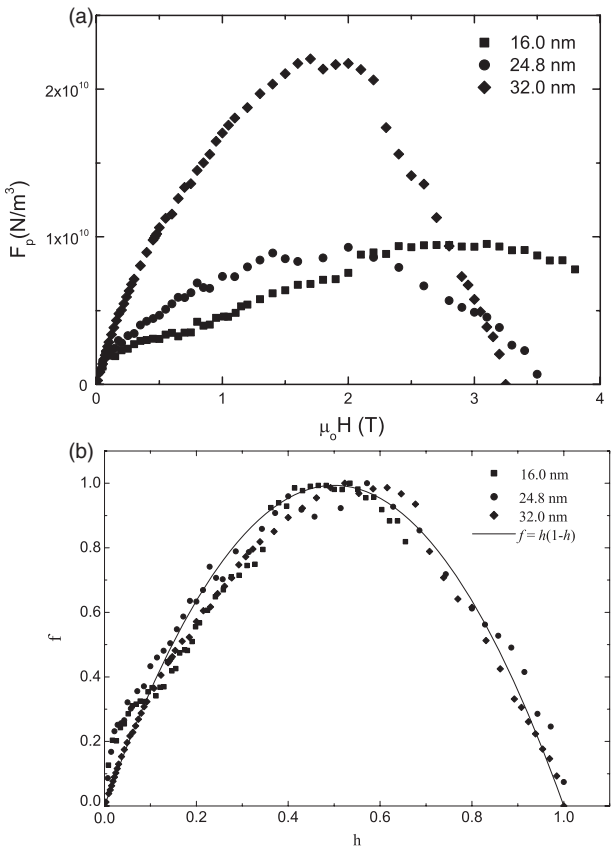

Figure 8. (a) Pinning force, F_p, versus parallel magnetic field, $\mu_0 H$, for samples with $d = 16$, 24.8 and 32 nm. (b) Reduced pinning force, f, versus reduced parallel magnetic field, h, for samples with $d = 16$, 24.8, and 32 nm (symbols). The solid line represents the law $f = h(1-h)$.

of the $J_c(d)$ dependence. In figure 8(a) we show the $F_p(H)$ dependence for the samples with $d \leqslant 32$ nm. In figure 8(b) the reduced pinning force, $f = F_p/F_{pmax}$, versus the reduced magnetic field, h, is reported for the same samples. From

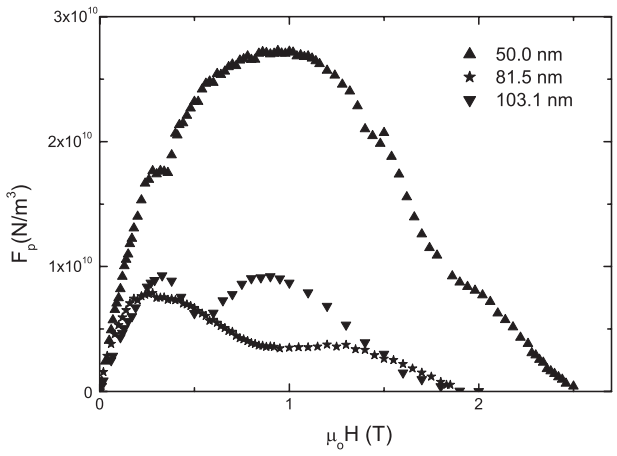

Figure 9. Pinning force, F_p, versus parallel magnetic field, $\mu_0 H$, for samples with dq = 50, 81.5 and 103.1 nm.

figure 8(b) it follows that the data have the same field dependence, described by the general scaling law $f = h(1 - h)$, shown in figure 8(b) as a solid line. This result indicates that we are in the presence of single vortex pinning [22].

In figure 9 we show the $F_p(H)$ dependencies for thicker films, $d \geqslant 50$ nm. These curves, which in this case present two maxima, do not correspond to the single pinning mechanism. The results of figures 8 and 9 indicate that, in our samples, some crossover occurs in the pinning mechanism for thicknesses between 32 and 50 nm, in good agreement with the value of d_c estimated from equation (1). In addition, the two maxima in the $F_p(H)$ dependence are more pronounced for thicker samples. For instance, for the film with $d = 103.1$ nm, a significant increase in the pinning force at $\mu_0 H \approx 0.9$ T is observed. For the sample with $d = 50$ nm, an absolute maximum of the pinning force is present at the same field. This value of the magnetic field corresponds to the average spacing between vortices $a_0 \sim (\phi_0/H)^{1/2} \sim 50$ nm, where ϕ_0 is the flux quantum. We believe that the maximum of the pinning force at this magnetic field is related to commensurability effects between the intervortex distance and the film thickness. In fact, for the sample with $d = 50$ nm at $\mu_0 H = 0.9$ T, vortices are located close to the film surfaces and surface pinning (favoured by surface roughness, which is present in our samples, as revealed by x-ray analysis) becomes essential, causing the very pronounced increase in the F_p value. For the film with $d = 103.1$ nm, the commensurability is also realized but, in this case, the film thickness is about twice the vortex lattice period, so that the outer vortices are pinned by the surfaces, while the internal vortices are intrinsically pinned. This explains the lower value of the maximum of the pinning force for this thicker sample. The observed large shoulder on the $F_p(H)$ dependence for the sample with $d = 81.5$ nm is also related to the commensurability effect. In this case, the commensurability field ($\mu_0 H = 0.13$ T), for which the vortex distance is half the layer thickness, is situated in the zone of decreasing F_p due to the vicinity of H_{c2}. For this reason, a plateau instead of a peak is obtained in the $F_p(H)$ curve.

4. Theory

In order to interpret our experimental data, we considered, for the sake of simplicity, the case in which no vortices flow in the superconductor. In this case, the value of the critical current is determined by the depairing current density, J_c^{dp}, which depends on the value of the critical field, H_{c2}, and on the penetration depth, λ: $J_c^{dp} \propto 0.54\ H_{c2}/\lambda$ [23]. The maximum current that can be sustained theoretically in pure Nb at $T = 0$ K is then $J_c^{dp}(0) \approx 2.8 \times 10^{12}$ A m^{-2} [24, 25], which is two orders of magnitude higher than the J_c measured in our samples. Nevertheless, we believe that our theoretical approach, even if simplified, can give useful information on our experimental data. In fact, we expect that, when vortex motion is not involved and then the commensurability effect can be excluded, the $F_p(H)$ curves should not show the two maxima for thicker films. If this is confirmed, the influence of commensurability in the measured $F_p(H)$ dependencies is then proved.

Let us consider a long and wide superconducting plate with a thickness of d in a magnetic field. The field is assumed to be parallel to the plate surface. A transport current I_t flowing through the plate is also parallel to the plate surface and perpendicular to the external field. The system of Ginzburg–Landau equations [25] has the form

$$\frac{4\pi}{c}\mathbf{j}_s = \frac{\psi^2}{\lambda^2}\left(\frac{\Phi_0}{2\pi}\nabla\theta - \mathbf{A}\right), \tag{2}$$

$$\nabla^2\psi - \left(\nabla\theta - \frac{2\pi}{\Phi_0}\mathbf{A}\right)^2\psi + \frac{1}{\xi^2}\left(\psi - \psi^3\right) = 0, \tag{3}$$

where $\mathbf{A}$ is the vector potential of the magnetic field ($\mathbf{B} = \mathrm{rot}\ \mathbf{A}$) and $\mathbf{j}_s$ is the current density in the superconductor. In accordance with Maxwell equations:

$$\mathrm{rotrot}\ \mathbf{A} = \frac{4\pi}{c}\mathbf{j}_s. \tag{4}$$

In general, the order parameter is written in the form $\Psi = \psi e^{i\theta}$, where ψ is the module and θ is the phase of the order parameter.

Let us consider a Cartesian coordinate system (x, y, z). Let the y and z axes lie in the plane of the plate surface (z is directed along the external magnetic field H). Then, the vector potential has only a y component $\mathbf{A} = \mathbf{e}_y A(x)$. Since the transport current flowing per unit of plate width I_t induces a magnetic field $H_I = 2\pi I_t/c$ on its surface, the total field near the plate surface is $H \pm H_I$. This defines the boundary conditions for equations (2) and (3). In addition, on the plate surfaces, we take the conventional boundary conditions for the order parameter [25]:

$$\left.\frac{d\psi}{dx}\right|_{x=0,d} = 0. \tag{5}$$

Using the measured sample parameters reported in table 1, the estimated BCS coherence length $\xi_0 = 4.7$ nm, a typical value of the London penetration depth at $T = 0$ K, $\lambda_L(0) = 34.3$ nm, and an electron–phonon free length at $T = 300$ K, $l_{ph}(300) = 2.75$ nm [26], we obtained the theoretical dependences shown in figure 10. We observe that

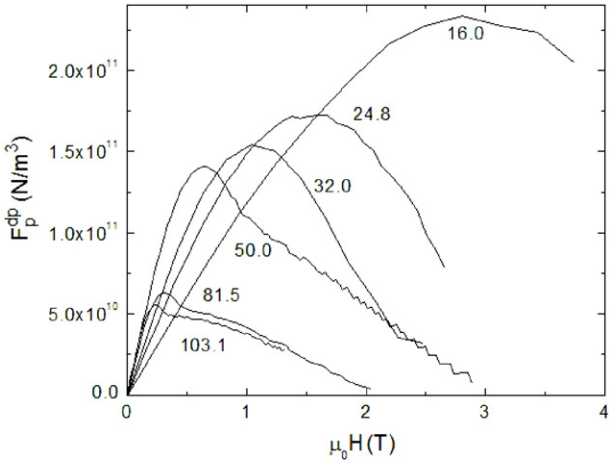

Figure 10. Theoretical $F_{\mathrm{p}}^{\mathrm{dp}} = |\boldsymbol{J}_{\mathrm{c}} \times \boldsymbol{H}|$ dependence versus parallel magnetic field, $\mu_0 H$, for all the samples. For details, see the text.

these curves do not show the presence of the two maxima in the case of thicker samples and that the critical current values are significantly higher with respect to the experimental ones. This is due to the different origin of the $F_{\mathrm{p}}(H)$ curves in the two cases. Our calculations are performed in the vortex-free limit [23]. However, in our experiment, vortices are present in the films and the critical current is also due to pinning. As a result, when the period of the vortex structure is equal to the film thickness, we have another local maximum in the $F_{\mathrm{p}}(H)$ and, in general, its absolute value is smaller. The results of our calculations also show that the upper critical magnetic field and the value of the maximum in the $F_{\mathrm{p}}(H)$ curves increases when decreasing the film thickness. In the vortex-free limit, the order parameter is suppressed only at the sample surface. In the case of thin films, this happens at any value of the external field [23]. In contrast, for thick films, the suppression of the order parameter happens only at low fields, because at high fields the order parameter and the current are located only at the film surface, giving rise to surface superconductivity in this case [23]. As a result, in this case, the $I_{\mathrm{c}}H$ product decreases at high magnetic fields.

5. Conclusions

In conclusion, the pinning properties of granular Nb films with different thicknesses were investigated in a parallel magnetic field. It was shown that the granularity of the films influences the $J_{\mathrm{c}}(\Theta)$ and $T_{\mathrm{c}}(\rho)$ dependencies. A crossover in the pinning regime was observed as a function of d, and the critical thickness d_{c} at which this changes occur was estimated. For thick films ($d > 32$ nm) a commensurability effect between the vortex structure and the film thickness was observed. The vortex-free case was analysed numerically on the basis of the Ginzburg–Landau equations solved for the case of a superconducting film in a parallel magnetic field. The comparison between the theoretical and experimental results confirms, for thicker films, the influence of the commensurability on the $F_{\mathrm{p}}(H)$ dependence.

Acknowledgments

ANL and AYT acknowledge financial support from the Ministry of Education and Science of the Russian Federation under State Contract no. 01.2.00 316542, the Russian Foundation for Basic Research (grant no. 06-02-17391) and the Russian Federal Support of Leading Scientific Schools.

References

[1] Cooper L N 1961 *Phys. Rev. Lett.* **12** 689
[2] Quateman J H 1986 *Phys. Rev.* B **34** 1948
[3] Park S I and Geballe T H 1985 *Physica* B+C **135** 108
[4] Golyamina E M, Dedyu V I, Lykov A N, Prischepa S L and Troyanovskii A M 1991 *Physica* C **185–189** 2031
[5] Saito Y and Anayama T 1973 *J. Appl. Phys.* **44** 5111
[6] Wördenweber R and Kes P H 1986 *Phys. Rev.* B **34** 494
[7] Stejic G, Gurevich A, Kadyrov E, Christen D, Joynt R and Larbalestier D C 1994 *Phys. Rev.* B **49** 1274
[8] Dew-Hughes D 1974 *Phil. Mag.* **30** 293
[9] Lykov A N 1993 *Adv. Phys.* **42** 263
[10] Sidorenko A S, Kolin'ko A E, Rybal'chenko L F, Cherkasova V G and Fogel' N Ya 1980 *Sov. J. Low Temp. Phys.* **6** 342
[11] Dedyu V I, Lykov A N and Prischepa S L 1990 *J. Exp. Theor. Phys.* **96** 872
[12] Koorevaar P, Maj W, Kes P H and Aarts J 1993 *Phys. Rev.* B **47** 934
[13] Tinkham M 1996 *Introduction to Superconductivity* (New York: McGraw-Hill)
[14] Parrat L G 1954 *Phys. Rev.* **95** 359
[15] Nevot L and Croce P 1980 *Rev. Phys. Appl.* **15** 761
[16] Als-Nielsen J and Mc Morrow Des 2001 *Element of Modern X-Ray Physics* (New York: Wiley)
[17] Face D W, Ruggiero S T and Prober D E 1983 *J. Vac. Sci. Technol.* A **1** 326
[18] Camerlingo C, Scardi P, Tosello C and Vaglio R 1985 *Phys. Rev.* B **31** 3121
[19] Golyamina E M, Dedyu V I, Lykov A N, Prischepa S L and Troyanovskii A M 1991 *Sverkhprovodimost'* **4** 1430
[20] Civale L *et al* 2004 *Appl. Phys. Lett.* **84** 2121
[21] Paranthaman M *et al* 2000 *J. Mater. Res.* **15** 2647
[22] Brandt E H 1980 *Phys. Lett.* A **77** 484
[23] Lykov A N, Tsvetkov A Yu and Zharkov G F 2005 *J. Exp. Theor. Phys.* **101** 341
[24] Rusanov A Y, Hesselberth M B S and Aarts J 2004 *Phys. Rev.* B **70** 024510
[25] Cyrot M and Pavuna D 1992 *Introduction to Superconductivity and High-T_{c} Materials* (Singapore: World Scientific)
[26] Alekseevskii N E, Nijankovskii V I and Bertel K H 1974 *Fiz. Met. Metalloved.* **37** 63